Journal of Electroceramics, 13, 727–732, 2004

Electrochemical Removal of NO_x by Scandium Doped Zirconia Membrane Reactor with Ceria Buffer Layer

HAE JIN HWANG,[1,*] JI-WOONG MOON[2] & MASANOBU AWANO[3]

[1] *Inha University, 253 Yonghyun-Dong, Nam-Gu, Incheon 402-751, Korea*
[2] *Korea Institute of Ceramic Engineering and Technology, 233-5 Gasan-Dong, GumCheon-Gu, Seoul 153-023, Korea*
[3] *Synergy Materials Research Center, AIST, 2268-1 Simo-shidami, Moriyama-ku, Nagoya 463-8687, Japan*

Submitted March 31, 2003; Revised February 16, 2004; Accepted June 29, 2004

Abstract. We developed a multi-layered LSCF/GDC/ScSZ/GDC/LSCF membrane reactor for NO decomposition, and its electrochemical properties and NO decomposition behaviors were investigated. A GDC buffer layer was able to prevent the harmful interfacial reaction between LSCF and ScSZ, mainly, strontium zirconate, which was observed in LSCF/ScSZ/LSCF membrane reactor. As a result, the electrode polarization resistance of the membrane reactor was significantly decreased in the multi-layered membrane reactor with the GDC buffer layer between the ScSZ electrolyte and LSCF electrode. From SEM observations, it was found that the GDC buffer layer deposited by a pulsed-laser deposition (PLD) process, was dense and showed homogeneous microstructure. Constructing the multi-layered membrane reactor could considerably reduce the consuming electrical power for NO decomposition.

Keywords: NO decomposition, LSCF, GDC, electrolyte, buffer layer, pulsed laser deposition, membrane reactor

1. Introduction

NO is a main cause of acid rain and air pollution, and it is said to be extremely harmful to the human body, leading to a respiratory disease or a disorder in a nervous system. Thus, NO emissions from automobiles and stationary combustion sources such as a boiler, power plants and so on are the serious problem, and solving the problem is a challenging task.

Some researchers have reported the electrochemical removal of NO using a solid electrolyte and porous electrodes [1–3]. When an electric current is applied to the cell, NO is directly decomposed at the cathode ($NO + 2e' + V_0^{\cdot\cdot} = O_O^x + 1/2N_2$). At the same time, oxygen ions are pumped through the solid electrolyte before evolving as oxygen gas at the anode, with the formation of oxygen vacancies ($O_O^x = 2V_O^{\cdot\cdot} + 2e' + 1/2\ O_2$). Such a cell can be used even in the presence of excess oxygen, with no aid of reducing agents like hydrocarbons.

*To whom all correspondence should be addressed. E-mail: hjhwang@inha.ac.kr

Recently, we have fabricated a dense GDC ($Gd_{0.2}Ce_{0.8}O_{3-\delta}$) membrane reactor coated by two symmetric porous LSCF ($La_{0.6}Sr_{0.4}Co_{0.2}Fe_{0.8}O_{3-\delta}$) catalytic electrodes for direct NO decomposition [4]. It is well known that LSCF is the most suitable electrode material for intermediate temperature applications, because of its high mixed (electronic and ionic) conductivity at the temperature range between 600 to 700°C, and excellent thermal and chemical compatibility to the GDC electrolyte [5, 6]. However, in our preliminary experiment, it was observed that the strength of the GDC electrolyte was considerably decreased after the current was applied to the membrane reactors. It seems that this results from the stress induced by a lattice expansion, which is associated with the partial reduction of Ce (IV) into Ce (III) in oxygen-deficient atmosphere [7, 8].

Sc_2O_3-doped ZrO_2 (ScSZ) would also be an attractive candidate as a solid electrolyte, due to its high ionic conductivity at the intermediate temperature range, 500° to 700°C, and good mechanical properties, for example, three-point bending strength; its ionic conductivity is approximately two or three times higher

than that of 8YSZ and comparable to that of GDC [9]. However, LSCF tends to react with ZrO_2, forming reaction products such as $La_2Zr_2O_7$ or $SrZrO_3$ [10, 11]. The materials chemically compatible with LSCF are CeO_2-based electrolytes, which have several disadvantages, as described just before. This would be the reason why we propose an LSCF/ScSZ/LSCF membrane reactor with GDC buffer layer between the ScSZ electrolyte and LSCF electrode for NO decomposition applications.

In this study, we fabricated a multi-layered membrane reactor for NO decomposition, which consists of ScSZ electrolyte, thin GDC buffer layer, and LSCF composite catalytic electrode. Pulsed laser deposition (PLD) was selected as a thin film processing for the GDC buffer layer. It is expected that dense and homogeneous thin GDC can be deposited on the ScSZ electrolyte. The electrochemical properties and NO decomposition characteristics of the membrane reactor were investigated.

2. Experimental Procedure

Two kinds of symmetrical membrane reactors were fabricated in this study; LSCF/ScSZ/LSCF, and LSCF/GDC/ScSZ/GDC/LSCF. The LSCF/ScSZ/LSCF was fabricated by screen-printing LSCF thick film electrodes (1.0 cm^2 in area) on both surfaces of a ScSZ electrolyte disk (89 mole% ZrO_2-10 mole% Sc_2O_3-1 mole% CeO_2, Japan Fine Ceramics Co. Ltd., Japan), and subsequently firing the membrane reactor at 1000°C for 2 h in air to form porous LSCF electrodes. The LSCF electrode includes 43 wt.% GDC (Anan Kasei Co. Ltd., Japan) in order to improve the electrochemical properties of the LSCF electrode [6]. The dimension of the ScSZ disk was 22 mm in diameter and 0.5 mm in thickness. The thickness of the LSCF electrodes was approximately 20 μm.

For the LSCF/GDC/ScSZ/GDC/LSCF membrane reactor, GDC buffer layers were deposited by pulsed laser deposition (PLD) process on both sides of the ScSZ disk before coating LSCF-GDC thick film electrodes. Spectron laser system Nd:YAG laser (wavelength of 355 nm, pulsed duration of 6 ns) was operated with a laser energy density of $\approx$8 J/cm^2 and laser frequency of 10 Hz on the GDC target. The GDC target used in this study was prepared by sintering the commercial GDC powder at 1400°C for 2 h in air. After the ScSZ substrate was mounted on the heater, the chamber pressure was reduced to approximately 2.0×10^{-4} Pa. The substrate was then heated to 700°C. Oxygen gas was introduced and the oxygen partial pressure increased slowly up to 1.5 Pa. The deposition of GDC was carried out at 600°C for 2 h. And then the obtained GDC thin film was heat-treated at 1000°C for 1 h in air.

The cathode and anode compartments were separated by the GDC electrolyte. The reactant gas, which is a mixture of 1000 ppm of NO and 2% of O_2 (balanced by He), from a pre-mixed gas cylinder was supplied to cathode at a flow rate of 50 ml/min. 21% of O_2 (balanced by He) was supplied to anode compartment at the same manner. Two Pt wires were contacted to the Pt current collecting layer. AC impedance spectroscopy was measured by a frequency analyzer (Model 1255B, Solartron) and NO decomposition characteristics were evaluated by applying a constant current to the membrane reactor using a galvanostat (Model 1286, Solartron) at 600°C. NO concentration in the effluent from the cathode compartments was determined with a chemiluminescent NO-NO gas analyzer (BSU-100 uH, Best Instrument). Microstructures were observed by scanning electron microscope (SEM, JSM-6320FK, JEOL Co. Ltd., Japan) and transmission electron microscope (TEM, Hitachi H-9000UHR III, Hitach Co. Ltd., Japan). For the characterization of crystalline phase of the PLDed GDC, an X-ray diffraction pattern was obtained with a powder diffractometer (RU-200B, Rigaku Co. Ltd., Japan).

3. Result and Discussion

Figure 1(a) and (b) shows cross section view of the LSCF/ScSZ/LSCF membrane reactor, and the detailed microstructure at the ScSZ/LSCF interface, respectively. It is evident from Fig. 1(b), the interfacial phase existed on the surface of the ScSZ electrolyte and its thickness was approximately 30–40 nm. If the LSCF is sintered on the ScSZ electrolyte, the reactions between zirconia and lanthanum oxide or strontium oxide result in the insulating interfacial layer, as is mentioned before [10–13]. Qui et al. have studied the interfacial reaction between (Ln, Sr)CoO_3 (Ln = Pr, Nd and Gd) or (Ln, Sr)(Co, Fe)O_3 (Ln = Gd, Nd, Pr, and La) and YSZ. $Ln_2Zr_2O_7$ and $SrZrO_3$ appeared after heating LSCO or LSCF and YSZ at 1000°C for 100 h, and their relative amount depended on the composition of LSCO or LSCF [13]. On the other hand, Tu et al. showed

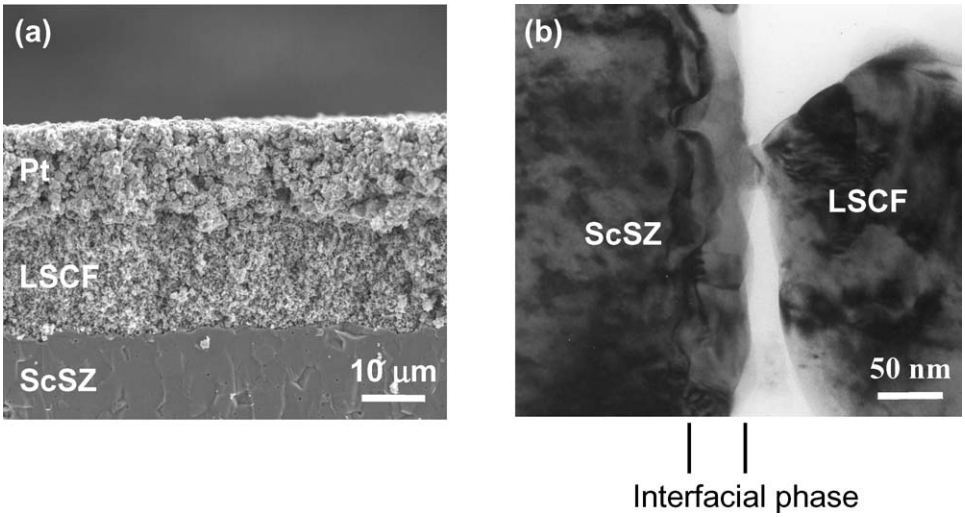

Fig. 1. Cross-section view showing the construction of LSCF/ScSZ/LSCF (a) and an interfacial phase between ScSZ electrolyte and LSCF electrode (b).

that the heat-treating $Ln_{0.4}Sr_{0.6}Co_{0.8}Fe_{0.2}O_{3-\delta}$ (Ln = La, Pr, Nd, Sm, and Gd) and 8YSZ mixtures at 900 and 1000°C for 96 h result in the production of only $SrZrO_3$ interfacial phase [10]. In this study, EDS analysis confirmed that its atomic composition was as follows; Sr 64.3%, La 2.1%, Fe 0.9%, Zr 14.5%, Sc 3.5%, and O 14.8%. Thus it can be inferred that SrO-based interfacial phase was mainly produced rather than La_2O_3-based one. Small amount of Fe and Sc diffusion from the LSCF electrode and ScSZ electrolyte was also detected, however, Co diffusion does not occur.

Brant et al. has addressed that the interfacial reaction phase between LSM and YSZ is lanthanum zirconate, $La_2Zr_2O_7$, for LSM with Sr content up to 30 mol% and, with increasing the Sr content, the formation of strontium zirconate, $SrZrO_3$ increasingly dominated [14]. In this study, the molar% of Sr in LSCF was 0.4, and thus it is reasonable that the main interfacial phase was found to be SrO-based one. The difference in the interfacial reaction products may be explained in terms of the composition of the ZrO_2 electrolyte. In the previous studies, Y_2O_3-stabilized ZrO_2 (YSZ) was used as an electrolyte, while we used Sc_2O_3- and CeO_2-stabilized ZrO_2. It seems that the presence of the Sc_2O_3 and CeO_2 in the ZrO_2 electrolyte can lead to different interfacial reaction mechanisms for LSCF and ScSZ, although the details of the reaction mechanisms are not clear.

In the case of the LSCF/GDC/ScSZ/GDC/LSCF membrane reactor, thin GDC buffer layer has been deposited on the ScSZ electrolyte in order to prevent harmful interfacial reaction between the ScSZ and LSCF. The thickness of LSCF composite electrode layer was estimated to be approximately 20 μm. The LSCF electrode sintered at 1000°C shows sufficiently porous and fine microstructure. It can be seen from Fig. 2 that the GDC buffer layer strongly adhered to the ScSZ electrolyte, and there were no cracks or a peel-off phenomenon between the electrolyte and GDC thin film.

Detailed microstructure of the GDC buffer layer prepared by PLD processes was shown in Fig. 2(b). The GDC buffer layer should be sufficiently dense because the ionic conductivity drops with increasing the porosity. A fully dense and uniform GDC buffer layer with thickness of approximately 2 to 3 μm has been successfully deposited on ScSZ substrate. Considering that the GDC and ZrO_2 reacts and interdiffuses during the sintering process at 1300°C [15], the PLD process is one of the suitable processes to fabricate a dense GDC thin film at the relatively low temperature. From the X-ray diffraction pattern obtained from the GDC thin film, it was confirmed that the GDC was well defined with a phase-pure cubic structure and all the peaks were corresponded to the GDC and ScSZ substrate.

EDS analysis of the PLDed GDC thin films gave information on the Gd and Ce atomic ratio. The differences in composition (Gd/Ce ratio) between the target and the deposited GDC thin film were minimized when

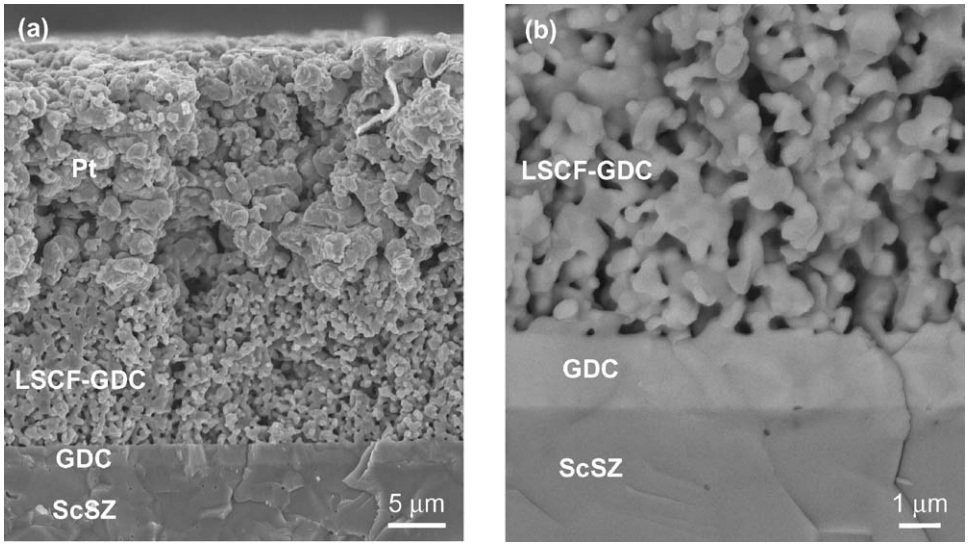

Fig. 2. Cross-section view showing the construction of LSCF/GDC (buffer layer)/ScSZ/GDC (buffer layer)/LSCF.

the oxygen partial pressure was 10 Pa, which was the highest oxygen partial pressure condition used in this study. Coccia et al. has been reported the GDC thin film deposition by PLD process [16]. According to their report, the Gd/Ce ratio of the as-deposited GDC thin film significantly deviated from that of the unablated target and the PLDed GDC thin film was Gd rich by a factor of two. Such a deviation may be due to the low oxygen partial pressure (approximately 10^{-3} to 10^{-1} Pa) during the ablation process.

Figure 3 shows impedance spectra, measured at 600°C in 2% oxygen atmosphere (balance He), of LSCF/ScSZ/LSCF (a) and LSCF/GDC/ScSZ/GDC/LSCF (b). For comparison, impedance spectra of some other membrane reactors (Pt/ScSZ/Pt and LSCF/GDC/LSCF) were also indicated in Fig. 3(b). Comparing with other membrane reactors, the polarization resistance of LSCF/ScSZ/LSCF was extremely high, as can be expected from TEM observation on the LSCF-ScSZ interface. On the other hand,

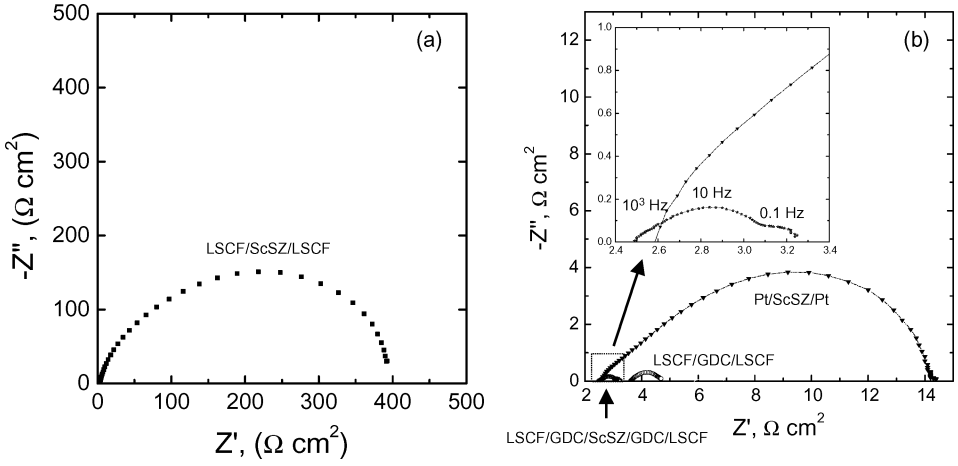

Fig. 3. AC impedance spectra of several membrane reactors used in this study. The operating temperature is 600°C.

LSCF/GDC/ScSZ/GDC/LSCF and Pt/ScSZ/Pt membrane reactors showed lower ohmic resistances than that of LSCF/GDC/LSCF, indicating that the bulk resistance of the ScSZ electrolyte is lower than that of the GDC electrolyte with the same geometric dimension.

Since the ionic conductivity of the ScSZ was estimated to be ∼0.02 S/cm at 636°C, the ohmic resistances should be 2.5 $\Omega \cdot cm^2$, on the assumption that the thickness of electrolyte was 0.5 mm and the resistance due to the LSCF electrodes and current collecting Pt layers can be ignored. As can be seen in Fig. 3(b), the ohmic resistances obtained in this study was 2.5 to 2.6 $\Omega \cdot cm^2$ at 600°C, which is almost similar with the calculated one, suggesting that our thin film processing and materials is adequately optimized.

The Pt/ScSZ/Pt electrochemical cell, which uses completely different electrode (Pt), shows poor electrocatalytic activity, and the polarization resistance with Pt electrode was 12 Ω. Considering the polarization resistance of the membrane reactors with LSCF electrode being 1 Ω, the LSCF electrode must to be one of the best electrode materials for the intermediate temperature applications, as is consistent to the papers reported by other researchers [5, 17]. The impedance spectrum for membrane reactor, LSCF/GDC/ScSZ appeared to be three depressed semicircles. In general, it was known that high and low frequency semicircles result from charge transfer- and diffusion-related processes, respectively [18]. As is evident in Fig. 3(b), low frequency semicircle peaked at 10 Hz was bigger than high frequency one at 10^3 Hz, indicating the electrode reaction being limited by charge transfer. The details of the electrode reaction mechanism are now under way.

As current flows through the membrane reactor, NO decomposes to nitrogen and oxygen ions on the cathode, and the oxygen ions can be pumped through the solid electrolyte to the anode [3]. Figure 4 shows NO decomposition behavior (NO concentration and pumped oxygen concentration curves) (a) and voltage curves (b) of two membrane reactors, as a function of the applied current. Irrespective of the reactor type, NO does not decompose approximately up to 200 mA. At 200–220 mA, NO starts to decompose and NO concentration abruptly decreases as the current increases. On the other hand, the pumped oxygen concentration linearly increases with increasing current. The dotted line in Fig. 4(a) is the oxygen concentration predicted by Faraday equation. The pumped oxygen concentration at a given current measured by on-line GC gave good agreement with the value that had been obtained by theoretical calculation, which means that the GDC or ScSZ electrolyte is a good electrolyte with no electronic conductivity.

As is evident in Fig. 4(a), NO concentration starts to decrease at the current at which 70–75% of oxygen included in the reactant gases had been pumped. Hibino et al. [3] have reported that NO starts to decompose after the oxygen has been pumped out below a certain level

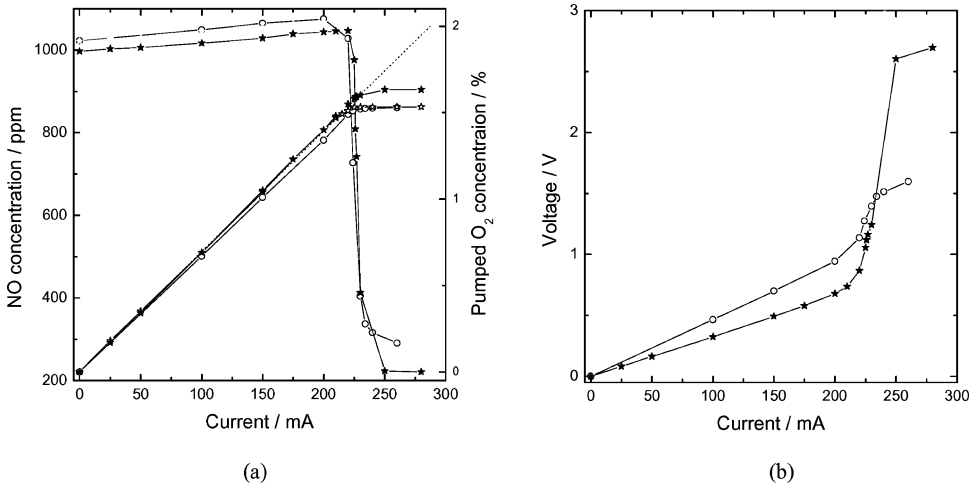

Fig. 4. NO decomposition and oxygen pumping behavior (a) and terminal voltage (b) as a function of the applied current for LSCF/GDC/LSCF (circles) and LSCF/GDC (buffer layer)/ScSZ/GDC (buffer layer)/LSCF (stars). The dotted line represents theoretical values calculated by Faraday equation. Reactant gas: 1000 ppm NO, 2% O_2 (He balance). Operating temperature: 600°C.

around the triple-phase boundaries, with the oxygen-pumping ability dependent on the affinity for oxygen of the triple-phase boundaries.

Another important mechanism responsible for the abrupt decrease in NO concentration may be associated with a ceria or zirconia (in ScSZ) reduction. The electrolyte reduction at low oxygen partial pressure results in oxygen vacancies with electron (F-centers) at around triple-phase boundaries, which may be another active site for NO decomposition. Huggins has addressed that electrochemically reduced zirconia electrolyte produces F-centers and it serves effective sites for NO decomposition [2]. As can be shown in Fig. 4, the onset current for NO decomposition was approximately 200 mA, at which pumped O_2 concentration curves are deviated from Faradiac equation, supporting that the electrolyte reduction make an important role to decompose NO. When the current exceeds the 220–230 mA, no further oxygen pumping occurred, indicating the depletion of oxygen in the LSCF cathode. It was found that the current that is required to initiate NO decomposition did not depend on the difference in the membrane reactor.

As can be expected from ohmic and polarization resistances of membrane reactors, the terminal voltage of LSCF/GDC/ScSZ/GDC/LSCF membrane reactor at a given current ranging from 0 to 220 mA was lower than LSCF/GDC/LSCF (Fig. 4(b)). The problem is why the voltage jump of the LSCF/GDC/ScSZ membrane reactor is so high above ∼220 mA. It is considered that this phenomenon may be associated with reduction of ScSZ electrolyte or GDC buffer layer. The consuming electrical power for NO decomposition would be considerably reduced by constructing the multi-layered membrane reactor, LSCF (cathode)/GDC (buffer layer)/ScSZ (electrolyte)/GDC (buffer layer)/LSCF (anode).

4. Conclusion

It was found that an SrO-ZrO_2-based interfacial phase formed at LSCF-ScSZ interfaces, resulting in the high electrode polarization resistance of the LSCF/ScSZ/LSCF membrane reactor, but not in the ohmic resistance. On the other hand, GDC buffer layer deposited by Pulsed laser deposition plays an important role to prevent the interfacial reaction between the ScSZ and LSCF. Therefore, it allows the use of LSCF with ScSZ electrolyte, lower both the ohmic and interfacial resistance, and enhance NO decomposition characteristics. The proposed membrane reactor, LSCF (cathode)/GDC (buffer layer)/ScSZ (electrolyte)/GDC (buffer layer)/LSCF (anode), could reduce the consuming electric power for NO decomposition. Although it is difficult to scale up and commercialize the PLD process, electron bean PVD or sol-gel techniques can be an alternative to deposit dense GDC buffer layer on the ScSZ electrolyte.

Acknowledgments

This work has been supported by METI, Japan, as part of the Synergy Ceramics Project. Part of the work has been supported by NEDO.

References

1. S. Pancharatnam, R.A. Huggins, and D.M. Mason, *J. Electrochem. Soc.*, **122**, 869 (1975).
2. T.M. Gur and R.A. Huggins, *J Electrochem.*, **126**, 1067 (1979).
3. T. Hibino, K. Ushiki, and Y. Kuwabara, *Solid State Ionics*, **98**, 185 (1997).
4. H.J. Hwang, J.W. Moon, and M. Awano, *J. Euro. Ceram. Soc.*, **24**, 1325 (2004).
5. E. Maguire, B. Gharbage, F.M.B. Marques, and J.A. Labrincha, *Solid State Ionics*, **127**, 329 (2000).
6. V. Dusastre and J.A. Kilner, *Solid State Ionics*, **126**, 163 (1999).
7. S.P.S. Badwal, F.T. Ciacchi, and J. Drennan, *Solid State Ionics*, **121**, 253 (1999).
8. A. Atkinson, *Solid State Ionics*, **95**, 249 (1997).
9. O. Yamamoto, Y. Arati, Y. Takeda, N. Imanishi, Y. Mizutani, M. Kawai, and Y. Nakamura, *Solid State Ionics*, **79**, 137 (1995).
10. H.Y. Tu, Y. Takeda, N. Imanishi, and O. Yamamoto, *Solid State Ionics*, **117**, 277 (1999).
11. . J.M. Ralph, J.T. Vaughey, and M. Krumpelt, in *Procedings of the 7th International Symposium on Solid Oxides Fuel Cells VII*, (2001) Vol. 2001-16, pp. 466–475.
12. S.P. Jiang, *Solid State Ionics*, **146**, 1 (2002).
13. L. Qiu, T. Ichikawa, A. Hirano, N. Imanashi, and Y. Takeda, *Solid State Ionics*, **158**, 55 (2003).
14. M.C. Brant and L. Dessemond, *Solid State Ionics*, **138**, 1 (2000).
15. A. Tsoga, A. Gupta, A. Naoumidis, D. Skarmoutsos, and P. Nikolopoulis, *Ionics*, **4**, 234 (1998).
16. L.G. Coccia, G.C. Tyrrell, J.A. Kilner, D. Waller, R.J. Chater, and I.W. Boyd, *Appl. Surface Sci.*, **96–98**, 795 (1996).
17. S.J. Skinner, *Fuel Cells Bull.*, (33), 6 (2001).
18. E.P. Murray, M.J. Sever, and S.A. Barnett, *Solid State Ionics*, **148**, 27 (2002).